Experimental study of the effect of a steady perimetric blowing at the rear of a 3D bluff body on the wake dynamics and drag reduction

Manuel Lorite-Díez[1], José Ignacio Jiménez-González[1], Carlos Martínez-Bazán[1], Luc Pastur[2], and Olivier Cadot[3]

[1] Departamento de Ingeniería Mecánica y Minera, Universidad de Jaén, Campus las Lagunillas, 23071 Jaén, Spain,
[2] Institute of Mechanical Sciences and Industrial Applications, ENSTA-Paris, Institut Polytechnique de Paris, 828 Bd des Maréchaux, F-91120 Palaiseau, France, luc.pastur@ensta-paristech.fr
[3] School of Engineering, University of Liverpool, Liverpool L69 3GH, UK

Abstract. In a perspective of active flow control of the bistable wake of a square-back Ahmed body, we show that the steady blowing through a perimetric slit at the rear of the body is not equivalent to a material rear perimetric cavity, the latter being able to suppress the bistable dynamics and symmetrize the wake flow, while the former cannot achieve any of these two features, indicating that steady perimetric blowing is not able to control the symmetric unstable steady solution of the system.

Keywords: Aerodynamics of 3D bluff bodies, bistable dynamics, drag reduction, wake flow manipulation.

1 Introduction

Ahmed-like bluff bodies are prototype models for ground vehicles commonly used for academic research on aerodynamics performance [1]. Three-dimensional rectangular blunt bodies are known to exhibit bistable dynamics involving two reflectional symmetry-breaking wake flows, depending on the body base aspect ratio, Reynolds number and ground clearance, among other parameters [2–4]. These wake topologies break the reflectional symmetry, being the wake deflected on one or the other side with respect to the symmetry plane, yielding permanent side loading on the body, with sudden reversals of the lateral force and increase of the drag [2].

The use of a perimetric rear cavity at the back of the body suppresses the bistable dynamics and achieves a drag reduction of up to 9%, by stabilizing the (presumably) symmetric steady wake flow [5, 6]. In an active flow control perspective, it would therefore be beneficial to design a fluidic equivalent of the material cavity. It is tempting to achieve this goal by steadily blowing air through a perimetric slit at the back of the body.

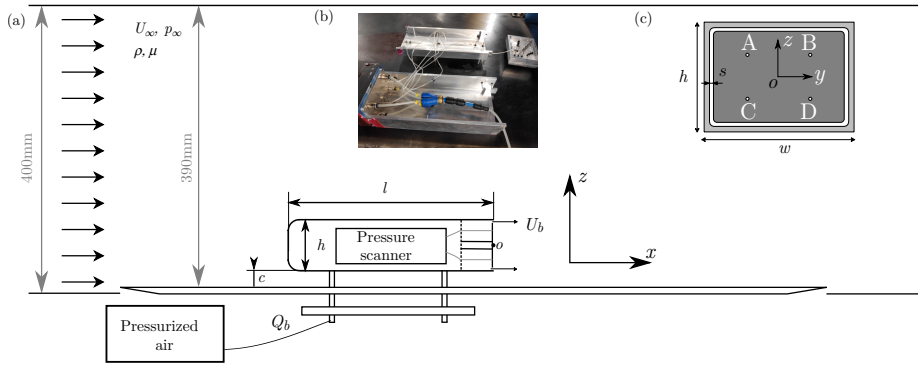

Fig. 1. (a) Sketch of the experimental setup with the body rear blowing system. (b) Picture of the body showing the feeding tubes for air blowing. (c) The back of the body with the pressure taps A, B, C, D.

Base blowing can suppress the periodic shedding at the wake behind axisymmetric bodies [7, 8]. It has been implemented in several experiments for open-loop and closed-loop control applications of the square-back Ahmed body wake flow [9, 10]. In these experiments, however, the unforced wake flow was either symmetric in the horizontal plane and only steadily deflected vertically [9, 10], or, when the flow was actually bistable in the horizontal plane, the control was shown to promote left/right transitions of the wake flow, only slightly decreasing the drag [10]. As a result, it could not be proved whether such a perimetric blowing actuator could stabilize or not the symmetric wake flow, associated with the lowest drag. The present contribution is aimed to experimentally test this question.

2 Experimental setup

A schematic view of the experimental set-up is shown in Fig. 1. A ground plate is placed in an Eiffel-type wind tunnel to form a 3/4 open jet facility, which provides a uniform stream of velocity $U_\infty = 20$ m/s, density ρ and dynamic viscosity μ. The turbulence intensity is smaller than 0.3% and the homogeneity of the velocity over the $390 \times 400\,\mathrm{mm}^2$ test section is about 0.4%. The Ahmed-like square-back model is $\ell = 291$ mm-long, $w = 97.25$ mm-wide and $h = 72$ mm-high. For this study, the ground clearance was set at $c/h = 0.278$.

Air blowing at the rear of the body is supplied through an additional frame of depth $d/h = 0.417$ whose internal cavity is pressurized by injecting a steady controlled flow rate Q_b of air through internal tubes, as shown in Fig. 1(b). This cavity is closed by a rear plate whose dimensions are adjusted such as to let a 2 mm-thick perimetric slit opened at the back of the body ($s/h = 0.028$), through which the rear base flow is discharged into the wake with velocity U_b.

The injected air flow rate Q_b is precisely controlled with a digital mass flow meter. The bleed coefficient is defined as $C_q = Q_b/U_\infty wh$.

The origin of the direct trihedral cartesian coordinate system (x, y, z) is placed at the center of the body base, being x the streamwise direction, z the direction normal to the ground and y the side direction. The characteristic length, velocity, pressure, and time scales are h, U_∞, $\rho U_\infty^2/2$ and h/U_∞, respectively. The Reynolds number $Re = \rho U_\infty h/\mu$ is set to 10^5.

The body base pressure is measured at probes A, B, C and D in Fig. 1(c), using a Scanivalve ZOC22 pressure scanner sampling at 100 Hz per channel over 250 s. The instantaneous pressure coefficient is defined as

$$c_p(y, z, t) = 2\left(p(y, z, t) - p_\infty\right)/\rho U_\infty^2,$$

where p_∞ denotes the reference static pressure at the inlet of the test section. The instantaneous base drag coefficient is calculated as

$$c_b(t) = -\sum_{M=\{A,B,C,D\}} c_p(M, t)/4,$$

and the wake asymmetry is evaluated by means of the gradients of the horizontal $g_y \approx h\left[(c_p(B,t) - c_p(A,t)) + (c_p(D,t) - c_p(C,t))\right]/2\Delta y$ and vertical $g_z \approx h\left[(c_p(A,t) - c_p(C,t)) + (c_p(B,t) - c_p(D,t))\right]/2\Delta z$ base pressure coefficients, with $\Delta y = y_B - y_A$ and $\Delta z = z_C - z_A$. Additionally, the drag force is measured through a multi-axial AMTI-MC3A load cell, while the recirculation bubble length L_r is estimated on the mean flow-fields obtained from PIV measurements in either the symmetric vertical plane or the horizontal mid-plane, using a dual pulse laser (Nd:YAG, 2×135mJ, 4ns) synchronized with a FlowSense 77 EO 4Mpx CCD camera.

3 Results

The first configuration we consider is the four-slit (4S) configuration. The sensitivity map of Fig. 2(a) shows that the perimetric steady blowing neither suppresses the wake asymmetry nor its bistability, for any value of the blowing coefficient C_q. Henceforth, the instantaneous wake flow remains either deflected to the left ($\hat{g}_y = -0.13$) or to the right ($\hat{g}_y = +0.13$) despite the blowing, with a higher probability for the later to occur at large C_q due to the blowing imperfect homogeneity. Meanwhile, the vertical gradient remains constant to $\hat{g}_z \approx 0.03$. However, as depicted in Fig. 2(b), the rear blowing has an impact on the time-averaged drag C_x, which is reduced by 3% for $C_q^\star \approx 6.6 \times 10^{-3}$, when the recirculation bubble is the most elongated. As also shown in Fig. 2(b), both the base drag C_b and the inverse of the recirculation length $1/L_r$ follow the same trend as the drag force. These correlated trends indicate that the rear-blowing first elongates the recirculating bubble, causing a pressure recovery at the base of the body as a consequence of the reduction of the bubble curvature and the associated pressure gradients, resulting in drag reduction, at small and moderate

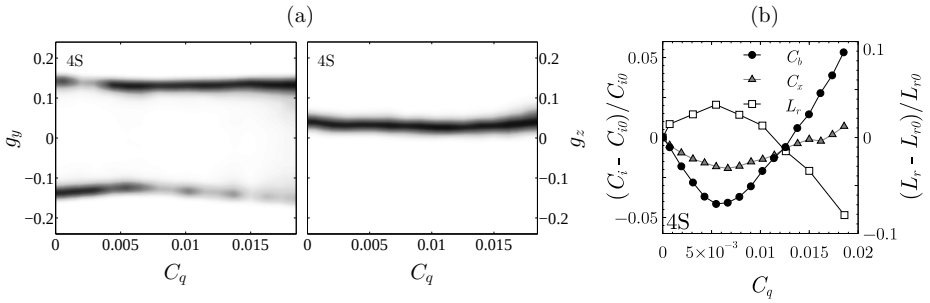

Fig. 2. (a) Probability distributions of the horizontal g_y and vertical g_z non-dimensional pressure gradients as the blowing coefficient C_q is increased (sensitivity map). White to black indicates unfrequent to frequent occurrences, respectively. The most probable values of g_y and g_z are $\hat{g}_y \approx \pm 0.13$ and $\hat{g}_z \approx 0.03$, respectively. The slight changes of g_y are presumably due to blowing non-uniformities. (b) Evolution of the relative variations of the time-averaged drag coefficient C_x, time-averaged base drag C_b and the recirculation bubble length L_r with C_q.

blowing flow rates [13]. In this regime, the rear-blowing therefore behaves like a steady base-bleeding actuation on the wake flow [11]. Meanwhile, the flow structure is smoothly adjusting to the new recirculation length, without significant modification, as shown in Fig. 3(a, b). For larger blowing flow rates beyond the optimal value $C_q^\star$, the bubble length decreases when increasing the blowing rate C_q, resulting in a base pressure decrease and consequently a drag increase. In this flow regime, the rear-blowing does not behave anymore like a base-bleed but instead contributes to the turbulent mixing in the shear layers.

As an interesting result, the body symmetry-preserving blowing of the four-slit configuration does not force the wake flow to recover its instantaneous symmetry. One may wonder whether this result remains true for any symmetric steady blowing configuration, namely the left and right (LR) blowing configuration, and, to a less extent, the top and bottom (TB) blowing configuration. The sensitivity map of Figs. 3(c, d) show that none of these two configurations can suppress the bi-stable dynamics of the wake flow. This also means that a symmetric steady blowing configuration at the rear of the body does not have the authority to stabilize the unstable symmetric wake flow solution.

4 Conclusion

Symmetric perimetric blowing with moderate flow rates at the rear of the bluff body has a beneficial impact on the drag, promoting an effective base-bleeding effect. However, unlike uniform base-bleeding, perimetric blowing is much easier to implement on real vehicles, offering new perspectives for practical applications. Interestingly, to the difference of a material cavity, perimetric blowing could not suppress the bi-stable dynamics of the wake flow, indicating that solid and fluidic-like rear cavities do not behave equivalently on the wake dynamics.

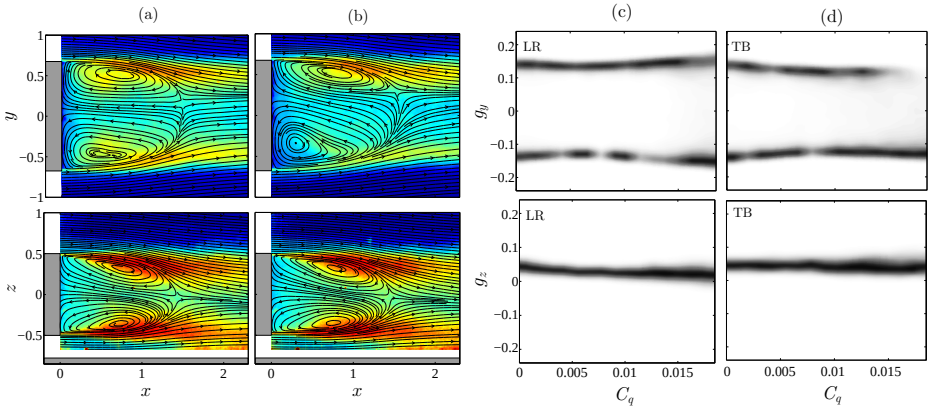

Fig. 3. (a,b) Mean flow field in the body symmetry vertical (top) and horizontal (bottom) planes without blowing (a) and at the optimal blowing flow rate $C_q^\star$ (b). The bubble length is defined as the outmost point in the flow field where the streamwise component of the velocity field u_x is negative. Statistical symmetry in the (xy) plane is recovered by averaging equi-probable mirror-conjugated flow states. (c,d) Probability distributions of the horizontal g_y and vertical g_z non-dimensional pressure gradients as the blowing coefficient C_q is increased (sensitivity map) in the left/right (LR) blowing configuration (c), top/bottom (TB) blowing configuration (d).

Acknowledgements. This work has been partially supported by the Spanish MINECO, MEDC and European Funds under project DPI2017-89746-R, José Castillejo Grant CAS18/00379 and Fellowship FPU 014/02945.

References

1. Choi H., Lee J., and Park H., Ann. Rev. Fluid Mech. 46, 441 (2014).
2. Grandemange, M., Gohlke, M., and Cadot, O., J. Fluid Mech. 722, 51 (2013).
3. Grandemange, M., Gohlke, M., and Cadot, O., Phys. Fluids 25, 095103 (2013).
4. Volpe, R., Devinant, P., and Kourta, A., Exp. Fluids 56, 99 (2015).
5. Evrard, A., Cadot, O., Herbert, V., D. Ricot, Vigneron, R., and Délery, J., J. Fluids Struct. 61, 99 (2016).
6. Sanmiguel-Rojas, E., Jiménez-González, J.I., Bohorquez, P., Pawlak, G., and Martínez-Bazán, C., Phys. Fluids 23, 114103 (2011).
7. Sevilla, A., and Martínez-Bazán, C., Phys. Fluids 16, 3460 (2004).
8. Bohorquez, P., Sanmiguel-Rojas, E., Sevilla, A., Jiménez-González, J.I., and Martínez-Bazán, C., J. Fluid Mech. 676, 110 (2011).
9. Barros, D., Borée, J., Noack, B.R., Spohn, A., and Ruiz, T., J. Fluid Mech. 805, 422 (2016).
10. Li, R., Barros, D., Borée, J., Cadot, O., Noack, B.R., and Cordier, L., Exp. Fluids 57, 158 (2016).
11. Bearman, P. W., Aero. Quarterly 18(3), 207-224 (1967).
12. Li, R., Bore, J., Noack, B. R., Cordier, L., Harambat, F., Phys. Rev. F 4(3), 034604 (2019).
13. P. W. Bearman, The Aero. Quart. Vol. XVIII, 207 (1967).